JOURNAL OF Materials Chemistry Communication

Fabrication of well-ordered macroporous active carbon with a microporous framework

Zhibin Lei,[a] Yugen Zhang,[b] Hua Wang,[a] Yanxiong Ke,[a] Jianmin Li,*[a] Fanqing Li[c] and Jinyun Xing[c]

[a]*Department of Chemical Physics, University of Science and Technology of China, Hefei, Anhui, 230026, P. R. China. E-mail: jmli@ustc.edu.cn*
[b]*Department of Chemistry, University of Science and Technology of China, Hefei, Anhui, 230026, P. R. China*
[c]*Structure Research Laboratory, University of Science and Technology of China, Hefei, Anhui, 230026, P. R. China*

Received 25th April 2001, Accepted 21st May 2001
First published as an Advance Article on the web 20th June 2001

Three-dimensionally ordered macroporous active carbon has been fabricated by carbonizing an aqueous solution of sucrose in the presence of sulfuric acid; nitrogen adsorption measurements show the presence of a microporous wall structure framework leading to a high BET surface area of 408 $m^2 g^{-1}$.

Materials with three-dimensionally ordered macroporous structure have recently been studied extensively because of their wide applications in separation, catalysis, optical information processing and microwave shielding.[1–4] These materials are created typically by template-directed methods. Colloidal crystals such as silica beads or polymer latexes are often the best templates used to prepare these materials. Depending on the method of introduction of materials into the interstices of templates, a number of methods have been developed for the fabrication of highly-ordered macroporous materials. These include sol–gel chemistry,[5–7] chemical vapor deposition (CVD),[8,9] electrochemical deposition,[10–15] thermal polymerization[16–19] and hydrodynamic infiltration of nanoparticles.[20] These methods have led to a wide range of macroporous materials, including ceramics,[5–7,21–23] semiconductors,[9] polymers[16–19] and metal films.[11–13]

One of the important applications of such materials is in catalysis and separation, for which abundant micropores and relatively high surface area are desirable. However, the surface area of macroporous materials so far has not exceeded 100 $m^2 g^{-1}$.[23] This is not surprising since large surface area is related to micro- or mesoporous structure. Investigation on the fabrication methods of well-ordered macroporous materials with microporous wall structures is an intriguing subject. For example, Holland *et al.* recently combined polystyrene spheres and a surfactant to fabricate macroporous silicates characterized by microporous silicate walls.[24] Due to the high number of micropores, the BET surface area of this macroporous material is high (421 $m^2 g^{-1}$). Lebeau *et al.* also synthesized ordered dye-functionalized mesoporous silica with macroporous architecture by similar dual templating.[25] As reported in this communication, without use of any surfactants, we have fabricated well-ordered macroporous active carbon by carbonizing an aqueous solution of sucrose in the presence of sulfuric acid. Similar pyrolysis methods have been used to fabricate highly-ordered carbon molecular sieves templated by MCM-48[26] and SBA-15.[27] Compared with previously reported methods for macroporous glass carbon, graphitic carbon and diamond[8] which were fabricated *via* a phenolic route, CVD and plasma-enhanced CVD, respectively, the present fabrication process is simple, cost-effective and time-saving. The macroporous carbon obtained shows long-range order and has a Brunauer–Emmett–Teller (BET) surface area of 408 $m^2 g^{-1}$. The large surface area suggests that this material should have promising applications in adsorption, separation and catalysis.

Nearly monodisperse SiO_2 spheres were synthesized by hydrolyzing tetraethoxyorthosilicate and subsequent seed growth polymerization under basic conditions.[28,29] The SiO_2 colloidal crystals can template self-assembly by the vertical deposition technique previously reported.[30] Before fabrication, the SiO_2 colloidal crystals were sintered at 820 °C for 3 hours.[31] This sintering endows the template with mechanical strength, as well as leading to small necks between neighboring spheres, which provide tunnels to allow HF solution to flow through the whole template. The carbon was introduced into the interstices of the template using the modified method of Ryoo *et al.*[26,27] Briefly, about 2 g SiO_2 template was added to a solution containing 2.5 g of sucrose, 0.15 ml of 98% H_2SO_4 and 10 ml of distilled water. The mixture was heated at 100 °C for 6 hours, followed by heating at 150 °C for a further 6 hours. Complete carbonization was accomplished by heating the composite in a tube oven *in vacuo* at 850 °C for 2 hours. The different carbon contents in Table 1 were controlled by changing the cycles of the whole carbonization procedure. The residual surface carbon was removed from the composite and the SiO_2 template was then etched away by overnight dissolution in 10% aqueous HF to leave behind a highly ordered macroporous active carbon. Elemental analysis (C, 98.4%; Si, 0.08%) indicates this treatment removes almost all the SiO_2 template and leads to a high-quality macroporous active carbon.

Fig. 1 shows scanning electron microscopy (SEM) images of the macroporous active carbon obtained after removal of the SiO_2 template. A regular hexagonal structure is clearly observed in Fig. 1B and C. Cross-sectional images showing well ordered structure (Fig. 1A) over large areas of *ca.* 4000 μm^2, indicate that the SiO_2 template was well replicated. By measuring the center-to-center distances between neighboring hollow spheres, an average shrinkage of 5% is evident. This shrinkage is much smaller than typically found for the sol–gel method.[5–7] Possible reasons for the shrinkage of the SiO_2 spheres are sintering or pyrolysis during the heating step which was performed before removal of the SiO_2 spheres by HF solution. The next lower layer of pores can also be seen in the high-magnification image of Fig. 1C. The small dark areas within each pore are the interconnected necks formed during the sintering and correspond to the points of contact of the starting SiO_2 spheres. It is interesting that the triangular

DOI: 10.1039/b103722f

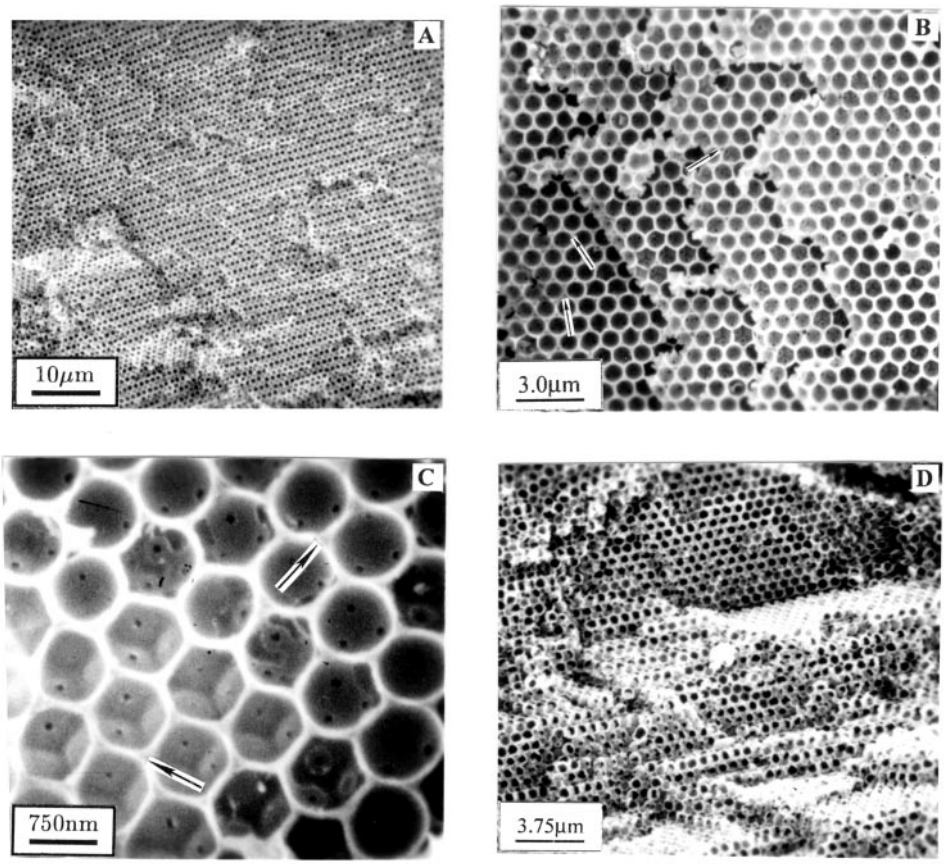

Fig. 1 SEM images of macroporous active carbon: (A) and (B) for sample 1, (C) and (D) for sample 2. (A) Cross-sectional image shows the long-range ordered structure over a large area of *ca.* 4000 μm^2. (B) Top-view image which suggests the carbon has retained the close-packed structure of the template. (C) High-magnification image of sample 2; the next lower layer is clearly seen. (D) Fracture-surface image of the fcc macroporous carbon. The multiple terraces indicate a periodic structure in three dimensions.

interstices (indiated by arrows in Fig. 1B and C) do not seem to be completely filled with carbon, although the pyrolysis time was prolonged and infiltration cycles were repeated. This indicates the macroporous carbon prefers to form by a surface-templated rather than a volume-templated process.[8] Multiple terraces, which are evident in the fracture-surface image of Fig. 1D, show that the interconnected walls extend the honeycomb structure in three dimensions.

The matrix of the wall structure of the macroporous carbon was also characterized by nitrogen adsorption measurements. The Barrett–Joyner–Halenda (BJH) pore volumes and BET surface areas of three samples were calculated and are listed in Table 1. Calculated from the desorption branches of the N_2 adsorption isotherms and the BJH formula, the average BJH pore diameter of three samples is *ca.* 3.4 nm, giving rise to a BET surface area as large as 408 $m^2\ g^{-1}$. In contrast to micro- and mesopores, macropores make little contribution to the total surface areas, see Table 1. Different carbon contents for the composite samples (Table 1) were observed upon varying the pyrolysis time and number of infiltration cycles. Assuming densities of 2.04 g ml^{-1} for SiO_2, 1.5 g ml^{-1} for carbon and that all available interstitial space between close packed SiO_2 spheres ($\sim$26%) was filled with carbon, then the mass fraction of carbon in the composite (carbon and SiO_2) would be 20.53%. The infiltration rates listed in Table 1 are based on this theoretically maximum value. For sample 1, a total single point pore volume of *ca.* 0.25 ml g^{-1} was measured while the BJH pore volume for pores >1.7 nm was 0.16 ml g^{-1}. The difference of about 0.1 ml g^{-1} can be ascribed to the microporous component of the active carbon with pores <1.7 nm. Large numbers of micro- and mesopores in the walls of the macroporous active carbon is of considerable interest for applications in catalysis and separation because they offer multiple benefits arising from each pore size regime. The micropores may provide size or shape-selectivity for guest molecules, while the additional macropores can offer easier transport and access to the active sites. Materials with bimodal pore systems show relatively short diffusion paths and therefore, are expected to improve reaction efficiencies and minimize blocking of channels.

In conclusion, we have fabricated well-ordered macroporous active carbon with a microporous framework under relatively

Table 1 Structure parameters of carbon/SiO_2 template composites and of macroporous active carbons after the SiO_2 template was removed

Sample	BET surface area/$m^2\ g^{-1}$	Pore volume[a]/ml g^{-1}	Macroporous diameter[b]/nm^{-1}	Carbon content[c] (%)	Infiltration rate[d] (%); cycles	Bulk density/g ml^{-1}	Porosity[e] (%)
Sample 1	408	0.16	871	5.37	26.2; 1	0.102	93
Sample 2	393	0.12	881	12.13	59.1; 3	0.230	85
Sample 3	408	0.15	240	6.53	31.8; 2	0.124	92

[a]Average BJH pore volume measured from the adsorption pore volume plot. [b]Determined from SEM images. [c]Carbon content determined from TGA in air refers to the carbon fraction in the composite (carbon and SiO_2 template). [d]Based on the theoretical maximum content of 20.53%. [e]Calculated from the bulk density, assuming a density of 1.5 g ml^{-1} for active carbon.

mild conditions. The hydroxyl and carboxylic groups within the micropores of the active carbon provide the possibility to graft various organic and inorganic functional groups. These structure properties as well as high surface area indicate that the macroporous active carbons fabricated in our work can be particularly useful as adsorbents for the removal of organic pollutants, as well as catalytic materials where mass transport is often hindered by small pore systems.

Acknowledgements

This work was financially supported by the National Natural Science Foundation of China and National Education Committee of China. Grant No. 20071030, 50072026 and 29871027.

Notes and references

1 E. Yablonovitch, *Phys. Rev. Lett.*, 1987, **58**, 2059.
2 Y. Xia, B. Gate, Y. Yin and Y. Lu, *Adv. Mater.*, 2000, **12**, 693.
3 C. M. Soukoulis, *Photonic Band Gap Materials*, Kluwer Academic Publishers, Dordrecht, 1996, vol. 315.
4 O. D. Velev and E. W. Kaler, *Adv. Mater.*, 2000, **12**, 531.
5 B. T. Holland, C. F. Blanford and A. Stein, *Science*, 1998, **281**, 538.
6 J. E. G. J. Wijnhoven and W. L. Vos, *Science*, 1998, **281**, 802.
7 Z. B. Lei, J. M. Li, Y. G. Zhang and S. M. Lu, *J. Mater. Chem.*, 2000, **10**, 2629.
8 A. A. Zakhidov, R. H. Baughman, Z. Iqbal, C. X. Cui, I. Khayrullin, S. O. Dantas, J. Marti and V. G. Ralchenko, *Science*, 1998, **282**, 897.
9 A. Blanco, E. Chomski, S. Grabtchak, M. Ibisate, S. John, S. W. Leonard, C. Lopez, F. Meseguer, H. Miguez, J. P. Mondia, G. A. Ozin, O. Toader and H. M. Driel, *Nature*, 2000, **405**, 437.
10 P. V. Braun and P. Wiltzius, *Nature*, 1999, **402**, 603.
11 P. Jiang, J. Cizeron, J. F. Bertone and V. L. Colvin, *J. Am. Chem. Soc.*, 1999, **121**, 7957.
12 P. N. Bartlett, P. R. Birkin and M. A. Ghanem, *Chem. Commun.*, 2000, 1671.
13 L. B. Xu, W. L. Zhou, C. Frommen, R. H. Baughman, A. A. Zakhidov, L. Malkinski, J. Q. Wang and J. B. Wiley, *Chem. Commun.*, 2000, 997.
14 H. W. Yan, C. F. Blanford, W. H. Smyrl and A. Stein, *Chem. Commun.*, 2000, 1477.
15 Z. Z. Gu, S. Hayami, S. Kubo, Q. B. Meng, Y. Einaga, D. A. Tryk, A. Fujishima and O. Sato, *J. Am. Chem. Soc.*, 2001, **123**, 175.
16 S. H. Park and Y. N. Xia, *Adv. Mater.*, 1998, **10**, 1045.
17 P. Jiang, K. S. Hwang, D. M. Mittleman, J. F. Bertone and V. L. Colvin, *J. Am. Chem. Soc.*, 1999, **121**, 11630.
18 B. Gates, Y. D. Yin and Y. N. Xia, *Chem. Mater.*, 1999, **11**, 2827.
19 T. Sumida, Y. Wada, T. Kitamura and S. Yanagida, *Chem. Commun.*, 2000, 1613.
20 O. D. Velev, P. M. Tessier, A. M. Lenhoff and E. W. Kaler, *Nature*, 1999, **401**, 548.
21 D. W. McComb, B. M. Treble, C. J. Smith, R. M. De La Rue and N. P. Johnson, *J. Mater. Chem.*, 2001, **11**, 142.
22 M. E. Turner, T. J. Trentler and V. L. Colvin, *Adv. Mater.*, 2001, **13**, 180.
23 H. W. Yan, C. F. Blanford, B. T. Holland, W. H. Smyrl and A. Stein, *Chem. Mater.*, 2000, **12**, 1134.
24 B. T. Holland, L. Abrams and A. Stein, *J. Am. Chem. Soc.*, 1999, **121**, 4308.
25 B. Lebeau, C. E. Fowler, S. Mann, C. Farcet, B. Charleux and C. Sanchez, *J. Mater. Chem.*, 2000, **10**, 2105.
26 R. Ryoo, S. H. Joo and S. Jun, *J. Phys. Chem. B.*, 1999, **103**, 7743.
27 S. Jun, S. H. Joo, R. Ryoo, M. Kruk, M. Jaroniec, Z. Liu, T. Ohsuna and O. Terasaki, *J. Am. Chem. Soc.*, 2000, **122**, 10712.
28 W. Stöber, A. Fink and E. Bohn, *J. Colloid Interface Sci.*, 1968, **26**, 62.
29 G. H. Bogush, M. A. Tracy and C. F. Zukoski IV, *J. Non-Cryst. Solids*, 1988, **104**, 95.
30 P. Jiang, J. F. Bertone, K. S. Hwang and V. L. Colvin, *Chem. Mater.*, 1999, **11**, 2132.
31 H. Miguez, F. Meseguer, C. Lopez, A. Blanco, J. S. Moya, J. Requena, A. Mifsud and V. Fornes, *Adv. Mater.*, 1998, **10**, 480.